Circulation: Arrhythmia and Electrophysiology

ORIGINAL ARTICLE

Human Induced Pluripotent Stem Cell–Derived Engineered Heart Tissue as a Sensitive Test System for QT Prolongation and Arrhythmic Triggers

Marc D. Lemoine, MD
Tobias Krause
Jussi T. Koivumäki, PhD
Maksymilian Prondzynski, MSc
Mirja L. Schulze, MSc
Evaldas Girdauskas, MD
Stephan Willems, MD
Arne Hansen, MD
Thomas Eschenhagen, MD
Torsten Christ, MD

BACKGROUND: Cardiac repolarization abnormalities in drug-induced and genetic long-QT syndrome may lead to afterdepolarizations and life-threatening ventricular arrhythmias. Human induced pluripotent stem cell–derived cardiomyocytes (hiPSC-CMs) should help to overcome the limitations of animal models based on species differences in repolarization reserve. Here, we compared head-to-head the contribution of I_{Ks} (long QT1) and I_{Kr} (long QT2) on action potentials (APs) in human left ventricular (LV) tissue and hiPSC-CM–derived engineered heart tissue (EHT).

METHODS: APs were measured with sharp microelectrodes in EHT from 3 different control hiPSC-CM lines and in tissue preparations from failing LV.

RESULTS: EHT from hiPSC-CMs showed spontaneous diastolic depolarization and AP generation that were sensitive to low concentrations of ivabradine. I_{Kr} block by E-4031 prolonged AP duration at 90% repolarization with similar half-effective concentration in EHT and LV but larger effect size in EHT (+281 versus +110 ms in LV). Although I_{Kr} block alone evoked early afterdepolarizations and triggered activity in 50% of EHTs, slow pacing, reduced extracellular K^+, and blocking of I_{Kr}, I_{Ks}, and I_{K1} were necessary to induce early afterdepolarizations in LV. In accordance with their clinical safety, moxifloxacin and verapamil did not induce early afterdepolarizations in EHT. In both EHT and LV, I_{Ks} block by HMR-1556 prolonged AP duration at 90% repolarization slightly in the combined presence of E-4031 and isoprenaline.

CONCLUSIONS: EHT from hiPSC-CMs shows a lower repolarization reserve than human LV working myocardium and could thereby serve as a sensitive and specific human-based model for repolarization studies and arrhythmia, similar to Purkinje fibers. In both human LV and EHT, I_{Ks} only contributed to repolarization under adrenergic stimulation.

VISUAL OVERVIEW: An online visual overview is available for this article.

Key Words: action potentials ■ E-4031 ■ HMR 1556 ■ induced pluripotent stem cell ■ ivabradine ■ long-QT syndrome ■ moxifloxacin

https://www.ahajournals.org/journal/circep

WHAT IS KNOWN?

- Human induced pluripotent stem cell–derived cardiomyocytes are a promising preclinical model to predict individual pharmacological responses, but there are concerns about immaturity.
- Incorporation of human induced pluripotent stem cell–derived cardiomyocytes into engineered heart tissue improves structural and electrophysiological maturation for example, cell orientation, cell-cell contact, upstroke velocity, and β-adrenergic response.

WHAT THE STUDY ADDS?

- Human induced pluripotent stem cell–derived cardiomyocytes–derived engineered heart tissues show greater action potential prolongation by I_{Kr} inhibition and by low-frequency pacing than human left ventricle working myocardium and are in this respect similar to Purkinje fibers.
- Human induced pluripotent stem cell-engineered heart tissues are sensitive to I_{Kr} block with common proarrhythmic compounds without being oversensitive to clinically safe compounds.

Impaired repolarization of cardiac action potentials (APs) is a critical factor in the development of early afterdepolarizations (EADs) and life-threatening arrhythmias. Long-QT syndrome (LQTS) is one such heritable arrhythmia disease, which is associated with prolonged QT because of a reduced repolarization reserve. The 2 most common LQTS types are caused by an impaired function of the slowly activating potassium current (I_{Ks}, LQT1) or the rapidly activating potassium current (I_{Kr}, LQT2) and cause ≈44% or ≈35% of all genetically identified LQTS, respectively.[1] Drug-induced LQTS is caused mainly by an unintentional I_{Kr} block. Therefore, new drugs have to be tested for their proarrhythmic potential. Nowadays, the compound effects on a single ion channel can be estimated in expression systems allowing automated measurements. However, the net effect on repolarization must be studied at AP level, especially if >1 channel is blocked by a compound.

Finding a valid model system to predict arrhythmia in humans is crucial for studying (drug induced) LQTS. Access to human ventricular tissue is limited and largely restricted to patients undergoing heart surgery with structural heart disease; accessing tissue with genetic proarrhythmic heart disease is nearly impossible. Therefore, animal models have been used to study the mechanisms of AP regulation in LQTS. Genetic heart disease can be studied in transgenic mice, but repolarization is remarkably different when compared with humans. The repolarization in mice is nearly independent of I_{Kr}. Heart tissue from larger mammals (rabbit, canine) is used for safety studies as their repolarization depends predominantly on I_{Kr}. The substantial interspecies differences in the contribution of individual repolarizing currents to AP duration (APD) regulation lead to different patterns of repolarization reserve.[2] For example, in canine left ventricle (LV), the I_{Kr} contribution is smaller than in nonfailing human LV. In guinea pigs, repolarization depends more on I_{Ks}, and the inhibition of a single component can be compensated by the remaining currents. Rabbit LV preparations display peculiarities in AP dynamics, such as AP shortening on low-frequency pacing in the physiological range of humans (<1.5 Hz),[3,4] which may disqualify rabbits as a universal model for human electrophysiology. Purkinje fibers (PFs) from rabbits are unique in their strong dependence on I_{Kr}, leading to marked AP prolongation[4] and EADs[5] in the presence of I_{Kr} blockers. Consequently, rabbit PFs are the most frequently used model in the pharmaceutical industry, where they are used to detect even small-QT-prolonging effects of new compounds suspected to block repolarizing currents.

It is expected that human induced pluripotent stem cell–derived cardiomyocytes (hiPSC-CMs) might overcome the problems of interspecies differences in animal models. The comprehensive in vitro proarrhythmia assay initiative was established to expand the understanding of torsadogenic mechanisms building on the emergence of new technologies with hiPSC-CMs. In addition, hiPSC-CMs open the possibility of studying genome-specific phenotypes of patients and could pave the way for individualized drug treatment. First, studies in hiPSC-CM generated from patients with monogenic arrhythmogenic diseases, for example, LQTS[6–8] and Brugada syndrome,[9] support this notion.

Still, there are concerns that hiPSC-CMs show a low degree of maturity, which may reduce the predictive value of this model for adult patients with cardiac diseases.[9–11] In the context of electrical stability, the repolarization reserve is not well characterized in hiPSC-CM since long-time AP measurements in single hiPSC-CM without artificial current injection or dynamic clamping are lacking.

Here, we use engineered heart tissue (EHT) to study the repolarization reserve of hiPSC-CM. This multicellular format allows the application of sharp microelectrodes[12,13] measuring APs without enzymatic dissociation. We evaluated CM from 3 different hiPSC lines cultured in EHT format in comparison to human LV muscle preparations. We then investigated whether hiPSC-CM may serve as a valid model for (drug induced) LQTS and whether it may be suitable as a sensitive test system for arrhythmic triggers.

METHODS

An expanded method section is available in the Data Supplement. Data, analytic methods, and study materials will be made available to other researchers for purposes of reproducing the results or replicating the procedures on request within the limits required for patient confidentiality.

Human Materials and hiPSC-CMs in EHT

This investigation conforms to all principles outlined by the Declaration of Helsinki and the Medical Association of Hamburg. All materials from patients were taken with informed consent of the donors. LV free wall samples were obtained from patients undergoing implantation of an LV assist device, heart transplantation, or aortic valve replacement. Patients having taken the medication amiodarone before the study were excluded. As previously described,[14] single cell suspensions of hiPSC-CM were subjected to EHT generation in a 24-well format (1×10^6 hiPSC-CM/EHT).

AP Measurements

APs were recorded as described previously[12,15] with standard sharp microelectrodes in intact EHTs (25–100 days old) or the endocardial site of LV tissue, which were field stimulated at 1 Hz at 50% above the stimulation threshold. AP parameters were stable for at least 60 minutes (Table I in the Data Supplement). We did not find a systematic influence of EHT culture duration on APD at 90% repolarization (APD_{90}), on effect size of E-4031 and HMR-1556 (Figure I in the Data Supplement), or on transcript levels of ion channels (Figure II in the Data Supplement). To measure rate adaptation, we allowed preparations to equilibrate for at least 500 beats before APD_{90} was measured. Short-term variability (STV) was calculated as previously described ($STV=\Sigma|APD_{90(n+1)}-APD_{90(n)}|/[30\sqrt{2}]$),[16] always in the absence of EADs.

Expression Analysis

Total RNA was extracted from snap-frozen LV and EHT using the RNAeasy mini Kit (Qiagen, CA). Fifty nanograms of total RNA was used for expression analysis (Table II in the Data Supplement) by NanoString nCounter SPRINT Profiler according to the manufacturer's instructions.

Statistics

GraphPad Prism 5 (GraphPad Software, San Diego, CA) was used for data analyses. Curves were fitted to data points from individual experiments, and all data were compared using unpaired or paired *t* tests when appropriate and for >2 groups 1-way ANOVA followed by Tukey corrections. All analyses were 2-tailed, and a $P<0.05$ was considered to be statistically significant. Group data are presented as mean±SEM.

Mathematical Modeling and Computer Simulations of CM Function

To test the influence of different ion current densities on the AP and repolarization reserve in hiPSC-CM, we used an established computer model for endocardial LV CM[17] and adjusted current densities based on previous publications (Table III in the Data Supplement).

RESULTS

AP Characteristics Under Basal Condition

All EHTs beat spontaneously with an average frequency of 1.19±0.10 Hz (n=40), whereas LV tissue was quiescent. To compare AP parameters (usually measured at 1 Hz), we selected EHT beating <1 Hz (27 of 40 EHTs). The AP shape in EHT was ventricular like, which could be quantified by a similar repolarization fraction ($[APD_{90}-APD_{50}]/APD_{90}$) in LV and EHT (0.26±0.01, n=34 versus 0.29±0.02, n=27; $P=0.07$; unpaired *t* test). Maximum diastolic potential (MDP; LV, –76.5±0.8 versus EHT, –77.4±1.2 mV; $P=0.53$), take-off potential (–77.0±0.9 versus –75.5±1.0 mV; $P=0.11$), AP amplitude (108.4±1.5 versus 105.8±1.8 mV; $P=0.11$), and maximum upstroke velocity (V_{max}: 230±17 versus 283±16 mV; $P=0.07$) did not differ between LV and EHT, but AP duration was shorter in EHT (APD_{50}, 165±13 versus 258±10 ms in LV, $P<0.001$; APD_{90}, 233±13 ms versus 343±9 ms in LV, $P<0.001$; Figure 1).

We compared the expression of genes coding for different ion channels in EHT (n=12) with LV (n=12; Figure 1C). All major repolarizing and depolarizing ion channels of LV were expressed in EHT. However, transcript levels of the channel subunit carrying the funny current (I_f; *HCN4*, 345±56 for EHT versus 64±7 for LV; $P<0.001$) and T-type calcium current (I_{CaT}; *CACNA1G*, 401±97 versus 13±2; $P<0.001$) were much higher in EHT than in LV. The expression of L-type calcium current (I_{CaL}; *CACNA1C*, 648±95 versus 380±40; $P=0.019$) and I_{Kr} subunits (*KCNH2*, 522±44 versus 388±34; $P=0.033$) was also higher in EHT than in LV, whereas those for I_{Na} (*SCN5A*, 969±133 versus 732±85; $P=0.15$), I_{Ks} (*KCNQ1*, 382±34 versus 309±40; $P=0.18$), and I_{K1} (*KCNJ2*, 355±82 versus 432±36; $P=0.40$) did not differ. Expression data for the 3 individual cell lines are given in Figure III in the Data Supplement.

Low Concentrated Ivabradine Allows Slow Pacing of EHT Without Affecting APD

Low beating frequency is necessary to unmask the large contribution of I_{Kr} to repolarization.[18] To slow down the beating rate in EHT (Figure 1B), we used the I_f blocker ivabradine. Even low concentrations of ivabradine (300 nmol/L) reduced spontaneous frequency effectively, as previously reported.[14] The beating frequency was reduced from 1.15±0.20 to 0.31±0.03 Hz (n=11; $P<0.001$; paired *t* test). At 1 Hz pacing, ivabradine reduced diastolic depolarization (DD) from 7.0±1.0 to 0.9±0.6 mV/s ($P<0.001$; paired *t* test; Figure 2). As a consequence, take-off potential was lowered (–75.3±2.2 to –79.5±2.5 mV; $P<0.01$) and AP amplitude increased from 109±2 to 116±2 mV ($P=0.017$), whereas upstroke velocity was not significantly raised from 302±27 to 360±47 V/s ($P=0.22$). MDP was not affected by ivabradine (from –82.6±1.3 to –82.3±1.3 mV). APD was neither affected by ivabradine in EHT (APD_{50}, 146±19 to 161±22 ms, $P=0.08$; APD_{90}, 224±23 ms to 242±28 ms, $P=0.20$) nor in LV (APD_{50}, 279±33 to 278±31 ms, $P=0.89$; APD_{90} 368±34 to 370±32 ms, $P=0.62$; n=5; paired *t* test; Figure IV in the Data Supplement).

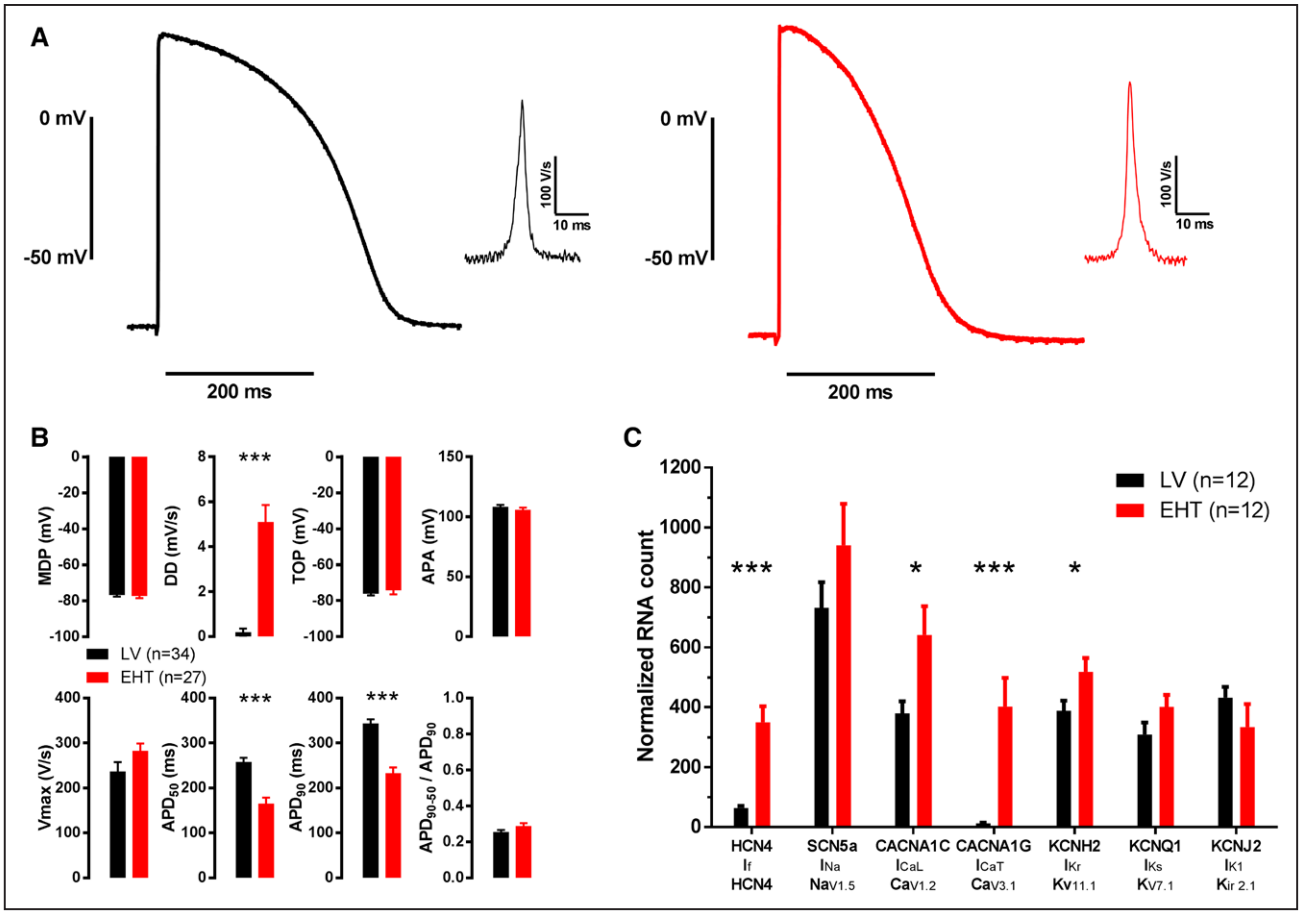

Figure 1. Basic characteristics of action potentials (APs) of human left ventricle (LV) and engineered heart tissue (EHT).
A, Representative examples of AP from LV (**left**) and EHT (**right**, in-house cell line C25). **B**, Summary of the results for maximum diastolic potential (MDP), diastolic depolarization (DD), take-off potential (TOP), AP amplitude (APA), maximum upstroke velocity (V_{max}), AP duration at 50% and 90% repolarization ($APD_{50/90}$), and repolarization fraction ($APD_{90\text{-}50}/APD_{90}$); n=number of preparations. **C**, Expression of various ion channel genes (mRNA) normalized to *GAPDH* and *PGK1* for LV and EHT. Mean±SEM, **P*<0.05, ****P*<0.001; unpaired *t* test.

Exaggerated Response to I_{Kr} Block in EHT

To test the contribution of I_{Kr} to the repolarization of hiPSC-CM in EHT, we used the I_{Kr} blocker E-4031. During AP measurements, all tissues were exposed to increasing concentrations of E-4031 (1 nmol/L to 1 µmol/L) in half-logarithmic steps (15 minutes incubation time per concentration step at 1 Hz pacing; Figure 3). E-4031 prolonged APD in all LV and EHT and slowed repolarization at membrane potentials <0 mV in LV and EHT. The half-effective concentration was not different between LV and EHT (73 nmol/L, n=8 versus 58 nmol/L in LV, n=12; *P*=0.42; Figure 3C). However, maximum prolongation of APD_{90} by E-4031 (measured at 1 µmol/L) was significantly larger in EHT (n=26) than in LV (n=14) in absolute and also relative terms (+281±18 versus +109±14 ms, *P*<0.001; +126±9% versus +37±5%, *P*<0.001). In a subanalysis of LV, APD_{90} was not significantly longer in tissues of female versus male patients (364±14 versus 324±12 ms; n=16 and 18; *P*=0.13), and there was no difference in APD_{90} prolongation on 1 µmol/L E-4031 (+121±22 ms, +35±8%, n=7 versus +107±19 ms, +38±8%, n=7; *P*=0.79; *P*=0.47). In the human heart, AP prolongation by I_{Kr} block is typically larger at slower beating rates (so-called reverse use-dependence).[3,18–20] Therefore, we studied the effects of E-4031 on APD_{90} at different pacing rates in a subset of experiments. The prolongation was larger at 0.5 Hz compared with 1 Hz in EHT (ΔAPD_{90}, +566±46 versus +273±35 ms, n=6; *P*<0.001) and in LV (ΔAPD_{90}, +176±42 versus +95±33 ms, n=6; *P*<0.001), demonstrating that both preparations have reverse use-dependence. However, the difference of ΔAPD_{90} at 1 and 0.5 Hz was bigger in EHT than in LV (+293±24 versus +81±22 ms; *P*<0.001) indicating a stronger reverse use-dependence of I_{Kr} block in EHT than LV.

We suspected that high I_{CaL} density in hiPSC-CM[21] contributes to pronounced AP prolongation by E-4031 in EHT. To test this hypothesis, we used verapamil to block I_{CaL}. Verapamil shortened APD in EHTs from 240±6 ms (basal) to 212±10 ms at 1 µmol/L (n=5; *P*=0.038). In the presence of 1 µmol/L verapamil, 1 µmol/L E-4031 prolonged APD to only 282±8 ms (n=5; Figure 4), which is significantly less prolongation (ΔAPD_{90}, +42±13 ms; Figure 4) than in the absence of verapamil (+218±18 ms, *P*<0.001; Figure 3B).

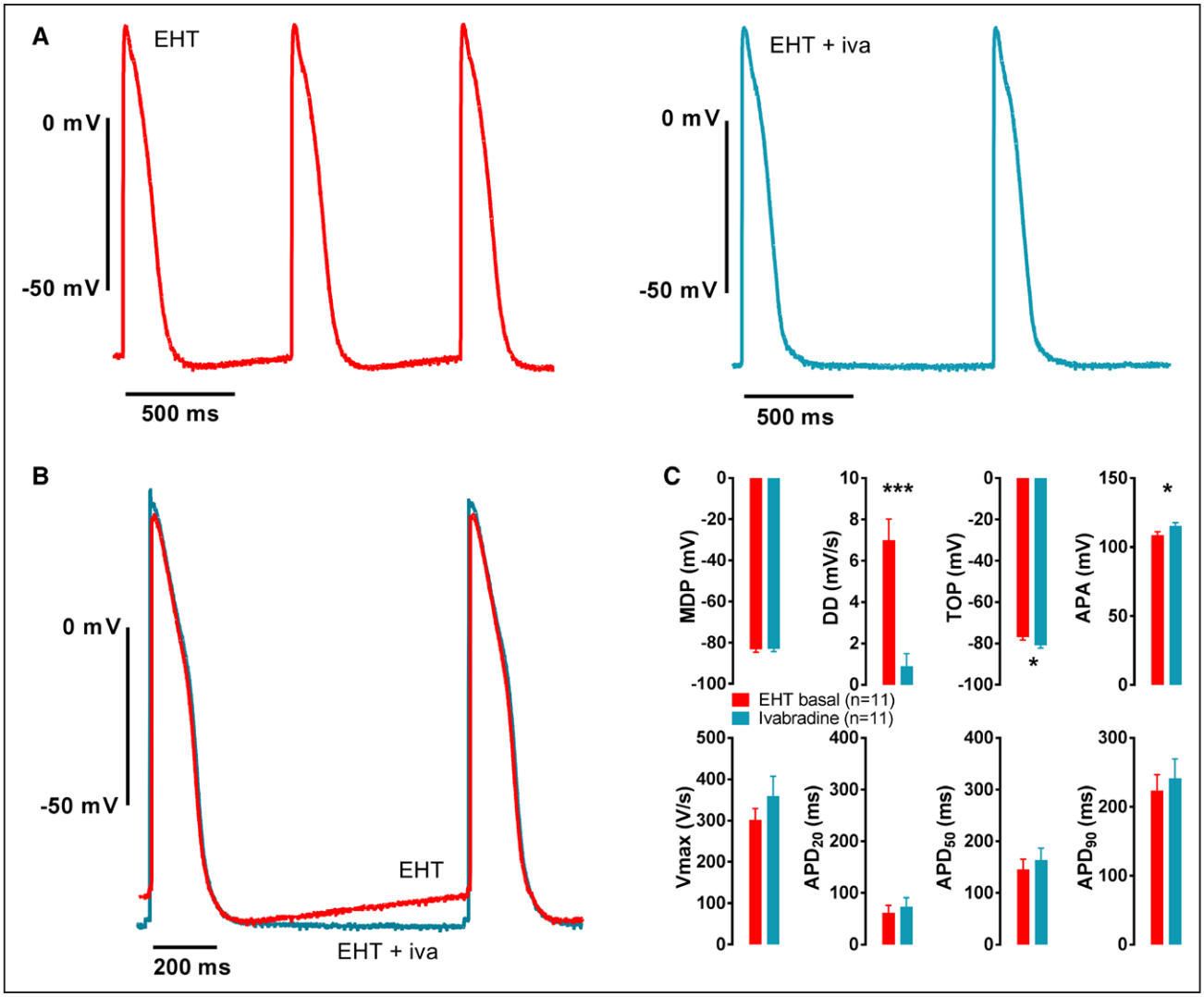

Figure 2. Effect of I_f block on diastolic depolarization (DD) in engineered heart tissue (EHT).
A, Representative action potentials (APs) of spontaneously beating EHT (in-house cell line C25) before (**left**) and after (**right**) exposure with 300 nmol/L ivabradine (iva). **B,** Superimposed APs from the same EHT paced at 1 Hz before (red) and after (turquoise) exposure to 300 nmol/L iva. **C**, AP parameters for EHT before (red) and after perfusion with 300 nmol/L iva (turquoise). Mean±SEM are shown for maximum diastolic potential (MDP), DD, take-off potential (TOP), action potential amplitude (APA), maximum upstroke velocity (V_{max}), and AP duration at 20%, 50%, and 90% repolarization ($APD_{20/50/90}$), *P<0.05, ***P<0.001; paired t test.

Minor Contribution of I_{Ks} to Repolarization Reserve in EHT

We used HMR-1556 as an I_{Ks} blocker. In human non-failing ventricle, contribution of I_{Ks} to AP is restricted to situations when repolarization reserve is reduced and β-adrenoceptors (β-ARs) are activated.[19] The same holds true for failing LV in our hands. APD_{90} was not prolonged by the I_{Ks} blocker HMR-1556 (1 µmol/L) alone (basal, 337±24 ms versus HMR-1556, 335±25 ms; n=9; P=0.87) and also not in EHT (248±43 versus 249±44 ms; n=7; P=0.77; paired t test; Figure 5). Even when repolarization reserve was reduced by pretreatment with E-4031 (1 µmol/L), HMR-1556 did not prolong APD_{90} significantly in LV (465±34 ms in E-4031 versus 476±41 ms in E-4031+HMR-1556; n=6; P=0.50; paired t test) or in EHT (526±49.0 versus 537±51 ms; n=4, P=0.20; Figure V in the Data Supplement). β-AR activation by isoprenaline (100 nmol/L) was necessary to demonstrate a prolongation of APD_{90} on HMR-1556 tested in the presence of E-4031 pretreatment in LV (428±29 ms in E-4031+isoprenaline versus 449±30 ms in E-4031+isoprenaline+HMR-1556, n=5; P<0.01) and EHT (496±38 ms in E-4031+isoprenaline versus 528±35 ms in E-4031+isoprenaline+HMR-1556; n=4; P=0.013; paired t test; Figure 5). The effect size of I_{Ks} block was small and did not differ between LV (+5.0±1.1%) and EHT (+6.6±1.7%; P=0.42; unpaired t test). In EHT, β-AR activation by isoprenaline (100 nmol/L) alone shortened APD_{90} (basal, 264±44 ms versus isoprenaline, 229±37 ms; n=5; P=0.033; paired t test) and consecutively administered HMR-1556 prolonged APD_{90} (isoprenaline, 212±52 ms versus isoprenaline+HMR-1556, 230±48 ms; n=3; P=0.048; paired t test, data not shown).

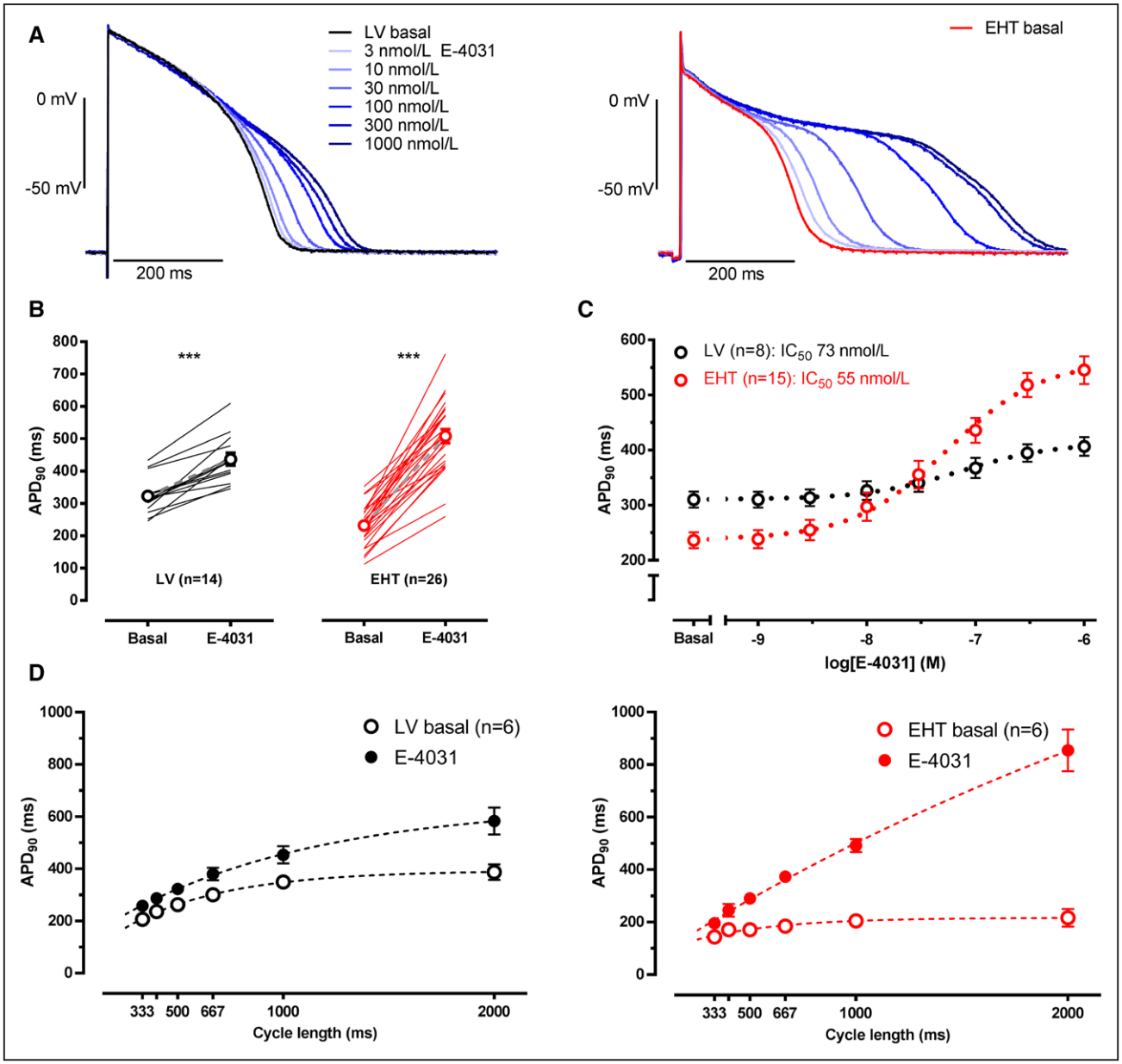

Figure 3. Effect of I_{Kr} block on repolarization in left ventricle (LV) and engineered heart tissue (EHT).
A, Original recordings of action potentials (APs) from LV (**left**) and EHT (**right**, in-house cell line ERC018) in the presence of increasing concentrations of E-4031. **B**, Effects of 1 µmol/L E-4031 on AP duration at 90% repolarization (APD_{90}) for LV (**left**, n=18) and EHT (**right**, n=32). Lines indicate individual responses, circles represent mean±SEM, ***P<0.001; paired t test. **C**, Concentration-response curves for the effect of E-4031 on APD_{90} in LV (black) and EHT (red). **D**, Frequency-dependent effect of 1 µmol/L E-4031 on APD_{90} in LV (**left**) and EHT (**right**). Mean±SEM.

Early Afterdepolarizations

The occurrence of EADs during in vitro testing is an alarming finding, suggesting a high probability of a drug to induce torsade de pointes (TdP). Therefore, we measured the inducibility of EADs and triggered activity in LV and EHT. I_{Kr} block alone by 1 µmol/L E-4031 was not sufficient to evoke EADs in LV (0/18), whereas EHTs developed EADs and triggered activity in 50% of cases (16/32; P<0.001, Fisher exact test). To induce EADs in LV, several additional interventions were necessary to reduce repolarization reserve (pacing rate at 0.33 Hz, lowering extracellular potassium from 5.4 to 2.7 mmol/L; β-AR stimulation with 100 nmol/L isoprenaline, I_{Ks} block with 1 µmol/L HMR-1556 and I_{K1} block by max; 300 µmol/L barium; Figure 6; Figure VI in the Data Supplement). Under these conditions, we could induce EADs in all 7 preparations of LV. In both, EHT and LV, EADs were preceded by incremental AP prolongation (Figure VII in the Data Supplement) or APD alternans (Figure 6). We analyzed APD_{90} of the last (or the second last in case of alternans) AP before the first EAD to define a critical APD value for EAD development. EHTs developed EADs at much shorter APD_{90} values than LVs (EHT, 531±49 ms, n=16 versus LV, 1072±63 ms, n=7; P<0.001; Figure 6B).

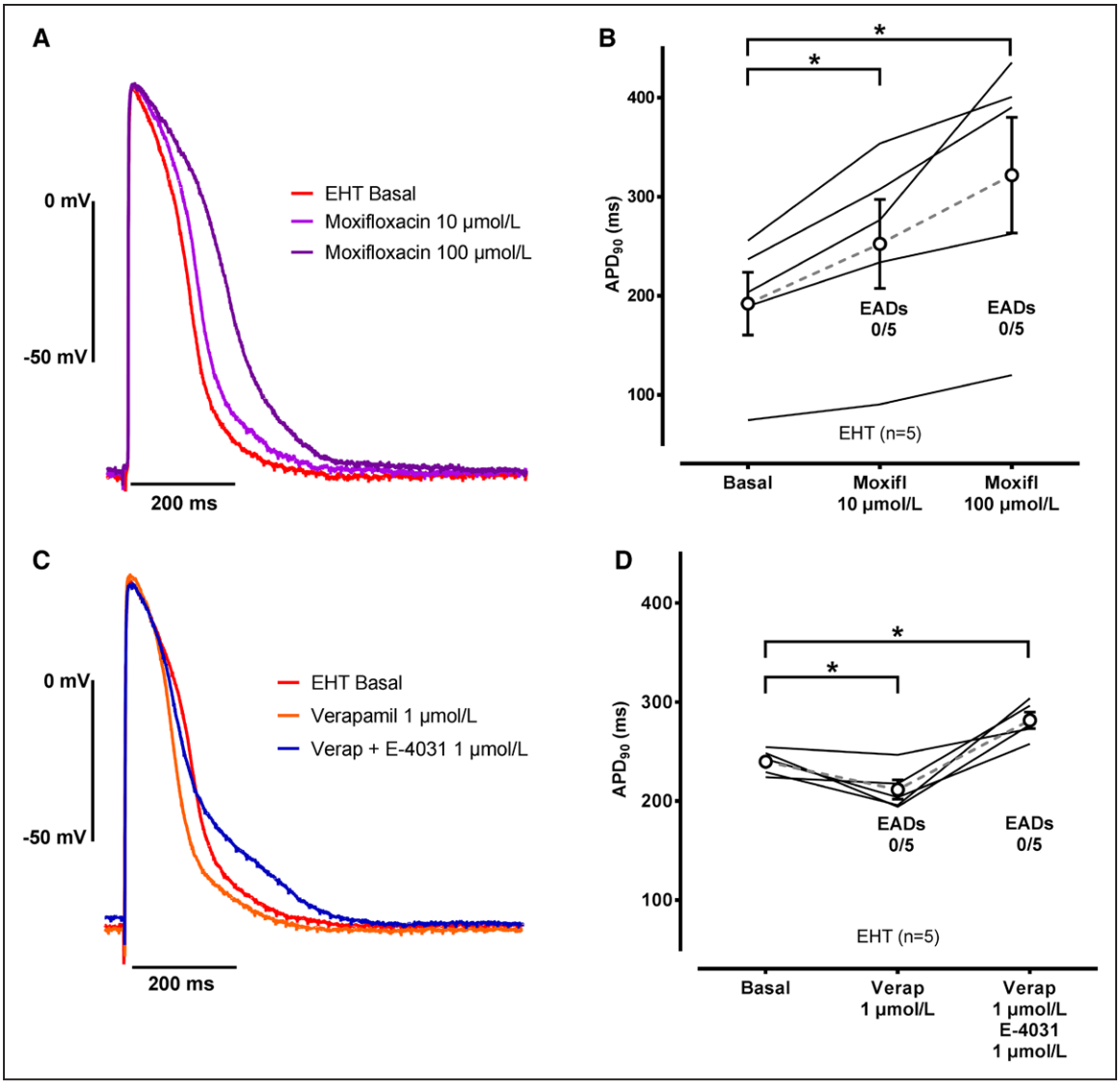

Figure 4. Effect of moxifloxacin and verapamil on action potential (AP) in engineered heart tissue (EHT).
A, Representative AP measurements of EHT (in-house cell line ERC018) at basal condition and with 10 and 100 µmol/L moxifloxacin. **B**, Effect of 100 µmol/L moxifloxacin on AP duration at 90% repolarization (APD_{90}). **C**, Representative APs of EHT (in-house cell line ERC018) with subsequently added 1 µmol/L verapamil (verap) and 1 µmol/L E-4031. **D**, Verapamil (1 µmol/L) and 1 µmol/L E-4031 on APD_{90} in EHT. Lines indicate individual responses, circles represent mean values±SEM (**B** and **D**), **P*<0.05 (paired *t* test). EAD indicates early afterdepolarization.

Specificity of EAD Development

Because test systems should provide not only a high sensitivity but also a high specificity, we tested 2 I_{Kr} blockers without proarrhythmic potential. Prior studies have shown that the antibiotic moxifloxacin induced EADs at 100 µmol/L in single CM but not in cardiac tissue or animal models.[22] In EHT, moxifloxacin prolonged APD_{90} from 202±36 ms (basal) to 252±52 ms at 10 µmol/L (*P*<0.01) and to 322±58 ms at 100 µmol/L (*P*=0.017; n=5) without the development of EADs (Figure 4). Verapamil is another I_{Kr} blocker without torsadogenic risk. In EHT, verapamil did not prolong APD or induce EADs (Figure 4), but reduced APD, in line with the well-known I_{CaL} blocking effect which seems to dominate at (clinically used) lower concentrations.

In-Silico Investigation of I_{Kr} Block and EADs

Simulation results obtained with adult CM and hiPSC-like CM in-silico models corroborated our experimental findings on I_{Kr} block (Figure 7). That is, AP prolongation was more pronounced in the hiPSC-like CM model than in the adult LV CM model. In line with our experimental findings, even a 100% block of I_{Kr} did not induce EADs in the adult CM model. In contrast, even incomplete block of I_{Kr} was sufficient to evoke EADs (Figure 7B) in the hiPSC-CM model. The new hiPSC-like CM model differs to the LV model in 4 current densities (4× I_{Kr}, 0.5× I_{K1}, 1.5× I_{CaL}, and additional I_{CaT}; Table III in the Data Supplement). Therefore, we tried to estimate individual contribution of each current to the low EAD threshold. We created 4 additional hiPSC-like CM models in which each current

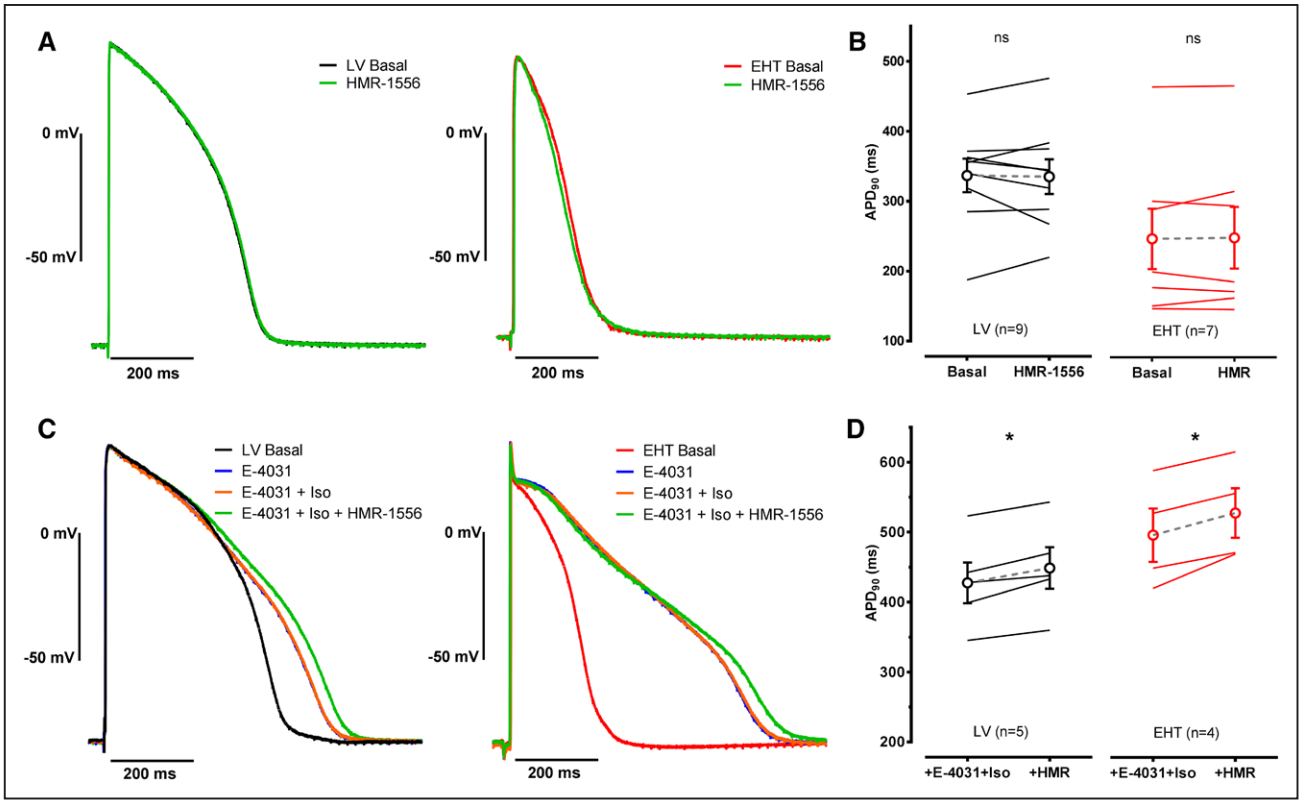

Figure 5. Effect of I_{Ks} block on action potential duration (APD) in left ventricle (LV) and engineered heart tissue (EHT).
A, Representative APs of LV and EHT (in-house cell line C25) before and after exposure to 1 µmol/L HMR-1556. **B**, Effect of 1 µmol/L HMR-1556 on APD at 90% repolarization (APD_{90}). Lines indicate individual responses, circles represent mean±SEM, paired *t* test. **C**, Representative APs of LV and EHT (in-house cell line C25) subsequently exposed to 1 µmol/L E-4031, 100 nmol/L isoprenaline (Iso), and 1 µmol/L HMR-1556. **D,** Effects of 1 µmol/L HMR-1556 on APD_{90} pretreated with 1 µmol/L E-4031 and 100 nmol/L Iso, mean±SEM, **P*<0.05; paired *t* test. ns indicates nonsignificant.

was separately reverted back to LV values (Figure 7C). In a next step, we applied increasing I_{Kr} block until the first EAD occurred (Figure 7D) to get a threshold value of I_{Kr} block to induce EAD. With LV I_{CaL} density,[21] APD of hiPSC-like CM was shorter (Figure 7C), and EAD development on I_{Kr} block was completely prevented (Figure 7D). Reverting I_{K1} or I_{CaT} density to adult values resulted in slight AP prolongation, but the EAD threshold of I_{Kr} block was only marginally lifted from 83% to 90% with adult I_{K1} density or to 86% without contribution of I_{CaT}. In contrast, the reduction of I_{Kr} density to LV level induced strong AP prolongation at basal condition and lowered the EAD threshold dramatically to 25% of I_{Kr} block.

Short-Term Variability

STV of APD ($STV=\Sigma|APD_{90(n+1)}-APD_{90(n)}|/[30\sqrt{2}]$) has been proposed as a parameter that predicts EAD development.[5] We compared the STV of APD_{90} in EHT and LV under baseline conditions and with E-4031 and formed subgroups of EHTs with and without EADs. At baseline, STV of APD_{90} did not differ between EHT and LV (1.46±0.38; n=14 versus 0.80±0.17; n=16; *P*=0.11; unpaired *t* test). STV was increased by E-4031 only in EHTs which subsequently developed EADs from 1.49±0.54 to 8.01±3.31 (n=7; *P*=0.049; paired *t* test), whereas LV and EHT without EADs showed no increase in STV (Figure 8). Moxifloxacin (100 µmol/L) did not increase STV in EHT (from 2.11±1.03 to 2.93±0.87; n=4; *P*=0.48; paired *t* test).

Differences Between hiPSC-CM Control Cell Lines

We designed this study with CMs from 3 different hiPS cell lines (2 academic: C25,hPSCreg name: TUMi001-A, and ERC018; and 1 commercial: iCell2), to identify general electrophysiological mechanisms of hiPSC-CMs. Although similarities prevailed, some aspects differed between cell lines (Figures III, VIII, and IX). ICell2 showed shorter APD_{20}, APD_{50}, and APD_{90} values than the other cell lines, as well as having higher mRNA levels of *SCN5A*, *CACNA1G,* and *KCNJ2* (Figure III in the Data Supplement). The AP shape differed between and within hiPSC-CMs of different lines. Figure VIII in the Data Supplement shows 3 representative APs for each cell line to illustrate individual differences in AP shape. Nevertheless, absolute AP prolongation on E-4031 was not different between hiPSC-CM cell lines (ΔAPD_{90}; C25, +303±37 ms; ERC018, +293±34 ms; iCell2, +248±20 ms), whereas each cell line showed a stronger prolongation than LV (ΔAPD_{90}, +114±14 ms; Figure IX in the Data Supplement).

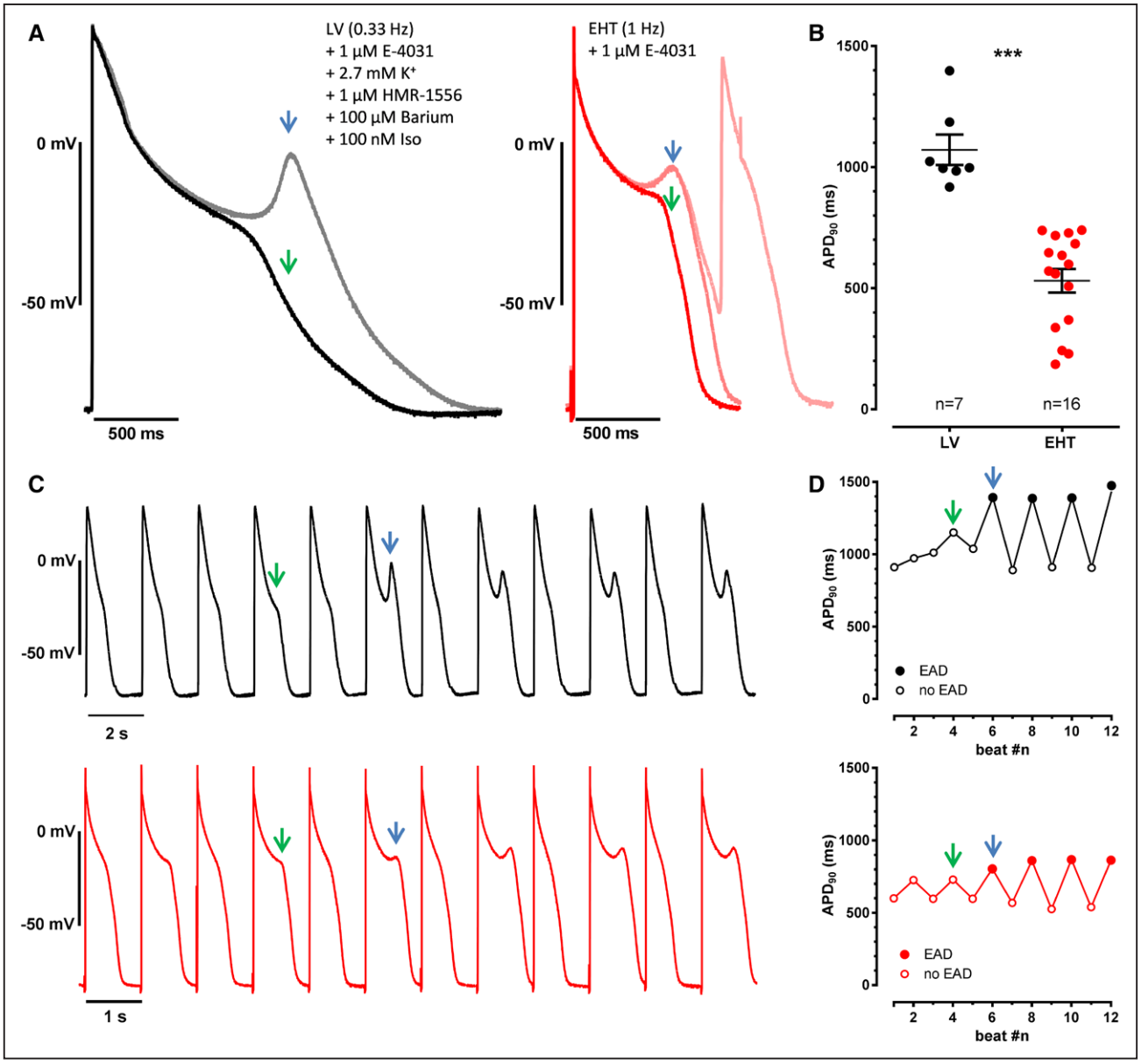

Figure 6. High susceptibility to early afterdepolarizations (EADs) and triggered activity in engineered heart tissue (EHT).
A, Original registrations of the first action potential (AP) with an EAD (blue arrow) and 2 beats before (green arrow) in left ventricle (LV) and EHT on LV and EHT (in-house cell line ERC018) exposed to 1 µmol/L E-4031, low potassium, 1 µmol/L HMR-1556, 100 µmol/L barium, and 100 nmol/L isoprenaline (LV) or to E-4031 only (EHT). **B**, AP duration at 90% repolarization (APD_{90}) for the longest AP before the first EAD in individual preparations; Mean±SEM for LV and EHT; ***P<0.001; unpaired t test. **C** and **D**, Development of EADs over time in LV (**top**) and EHT **(bottom**, in-house cell line ERC018). **C**, Series of APs showing APD prolongation/alternans and subsequent EAD development, same experimental conditions as in (**A**). Please note the different x axis scaling because slow pacing was necessary to induce EADs in LV. **D**, Quantification of APD_{90} shown for the corresponding AP sequence (**C**).

DISCUSSION

The study compared AP characteristics and responses to repolarization-slowing drugs in hiPSC-CM–derived EHTs and human LV muscle preparations. The main results were (1) that the I_f blocker ivabradine at low concentrations is an effective tool to reduce DD and spontaneous beating rate in hiPSC-CM–based EHTs without affecting repolarization, (2) that similar to human LV, the contribution of I_{Ks} to repolarization in EHT was detectable only in the presence of β-adrenergic stimulation and concomitant I_{Kr} inhibition, and (3) that EHT showed exaggerated AP prolongation, stronger reverse use-dependence, and a high susceptibility to EADs on I_{Kr} block when compared with human LV revealing a high sensitivity and specificity for arrhythmic triggers.

Ion Channel Expression and Basic Characteristics of APs

The repolarization fraction of APs, that is, the relation between early and late repolarization, was similar in EHT

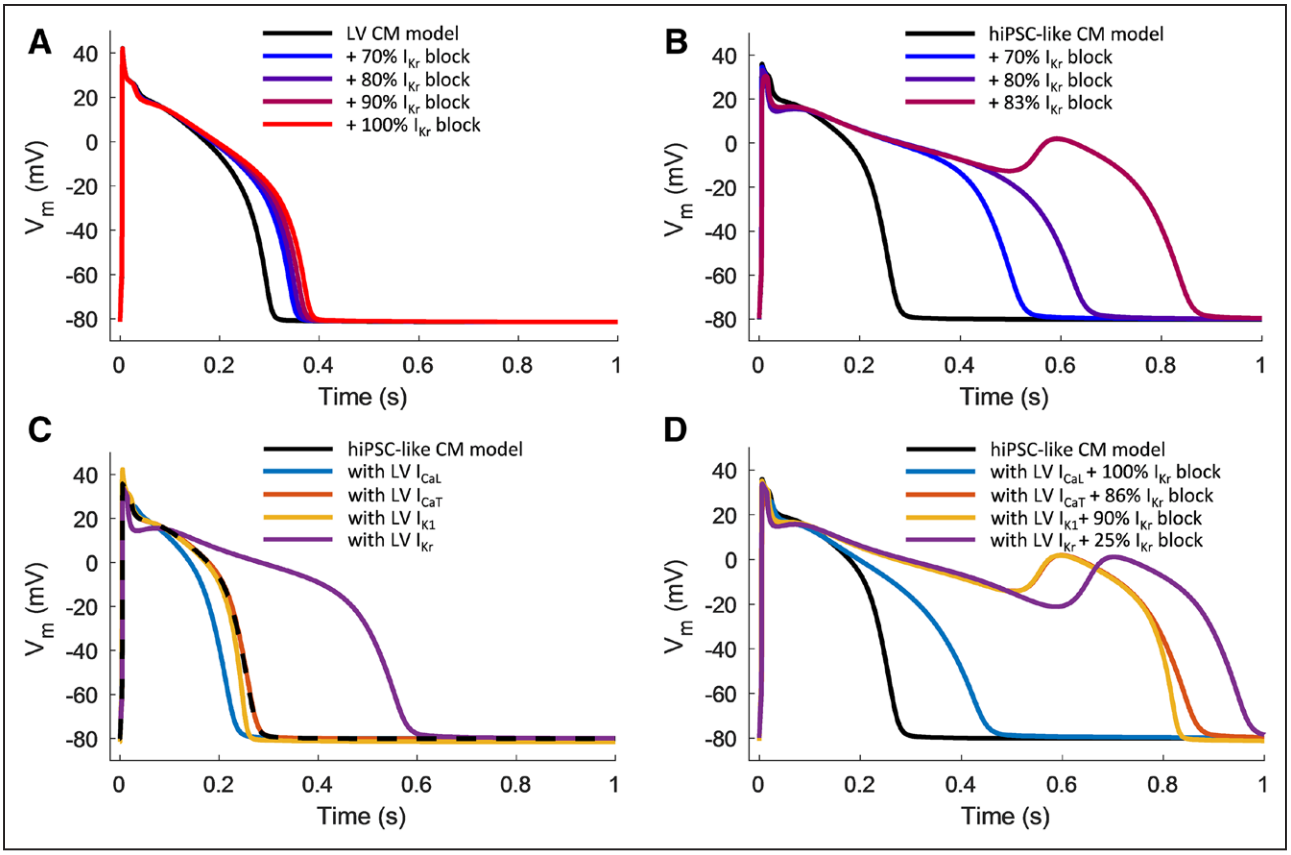

Figure 7. Simulated effect of I_{Kr} block on action potential (AP).
A, Effect of increasing I_{Kr} block in the standard in-silico model of human left ventricular cardiomyocytes (LV CMs) and in a modified human induced pluripotent stem cell–derived (hiPSC)–like cardiomyocytes (CM) in-silico model (**B**) with 1.5-fold I_{CaL}, 0.5-fold I_{K1}, 4-fold I_{Kr} density, and additionally implemented I_{CaT}. Early afterdepolarizations (EADs) appeared on 83% block of I_{Kr}. **C**, Human induced pluripotent stem cell–like CM model with separately reverted current densities of I_{CaL}, I_{K1}, I_{Kr}, and I_{CaT} to values as in LV. **D**, Computer calculation as in (**C**) with critical I_{Kr} block (in %) reaching threshold for EAD development. Please note that in case of LV I_{CaL} even 100% I_{Kr} block does not induce EAD.

and LV, suggesting that hiPSC-CM display a rather uniform ventricular-like repolarization pattern in EHT. On the other hand, automaticity of EHTs driven by DD is the most obvious electrophysiological difference in comparison to the quiescent LV tissues. A strong expression of *HCN4* (Figure 1), high current densities,[11] and the effectiveness of ivabradine on DD and beating frequency (Figure 2) indicate a relevant contribution of I_f to spontaneous pacemaking in hiPSC-CM. The robust expression level of *SCN5A* in EHT reflects the high I_{Na} density in hiPSC-CM[12] and the fast upstroke velocity, although DD slightly depolarizes the take-off potential and, thereby, reduces the functional availability of Na^+ channels. The high expression levels for I_{CaT} conforms with recent current recordings.[21] This I_{CaT} current may be relevant because the coexistence of $I_{Ca,L}$ and $I_{Ca,T}$ should generate more window Ca^{2+} current[21] during the plateau phase, increasing depolarizing forces and thereby reducing the repolarization reserve.

We found higher expression levels of *KCNH2* in hiPSC-CM than in LV in line with the higher I_{Kr} densities reported for hiPSC-CM (0.55–1.9 pA/pF)[6,7,11] versus LV (0.25–0.31 pA/pF).[2,23,24] Why differences in I_{Kr} density between hiPSC-CM and LV are more pronounced than those in transcript levels remains unclear. The expression of *KCNQ1* was similar, which is in line with I_{Ks} densities reported in a similar range for hiPSC-CM (0.3–1 pA/pF)[6,11,25,26] and LV (0.2–0.6 pA/pF).[2,27,28] As reported previously,[12] we measured physiological MDP in EHT corresponding to similar expression levels for *KCNJ2* in EHT and LV. Although I_{K1} densities are consistently reported to be 2- to 8-fold lower in hiPSC-CM (–0.85 to 2.9 pA/pF)[10,11,29] than in human LV (6–7 pA/pF)[2,23,30] at similar conditions (at –100 mV with 5.4 mmol/L K^+), several groups have measured physiological MDP <–74 mV[11,29,31] in hiPSC-CMs. This is in line with in-silico investigations, which suggests only a minimal depolarization of MDP if I_{K1} density is reduced by half in hiPSC-CM (Figure 7) and in LV.[2] These data underline that the contribution of I_{K1} to MDP is smaller than often anticipated.[13]

Low Concentrations of Ivabradine Allow AP Recording in EHT at Slow Rate

We have tried to reduce the spontaneous beating rate of EHT via pharmacological intervention because the effect of ivabradine on spontaneous beating frequency of

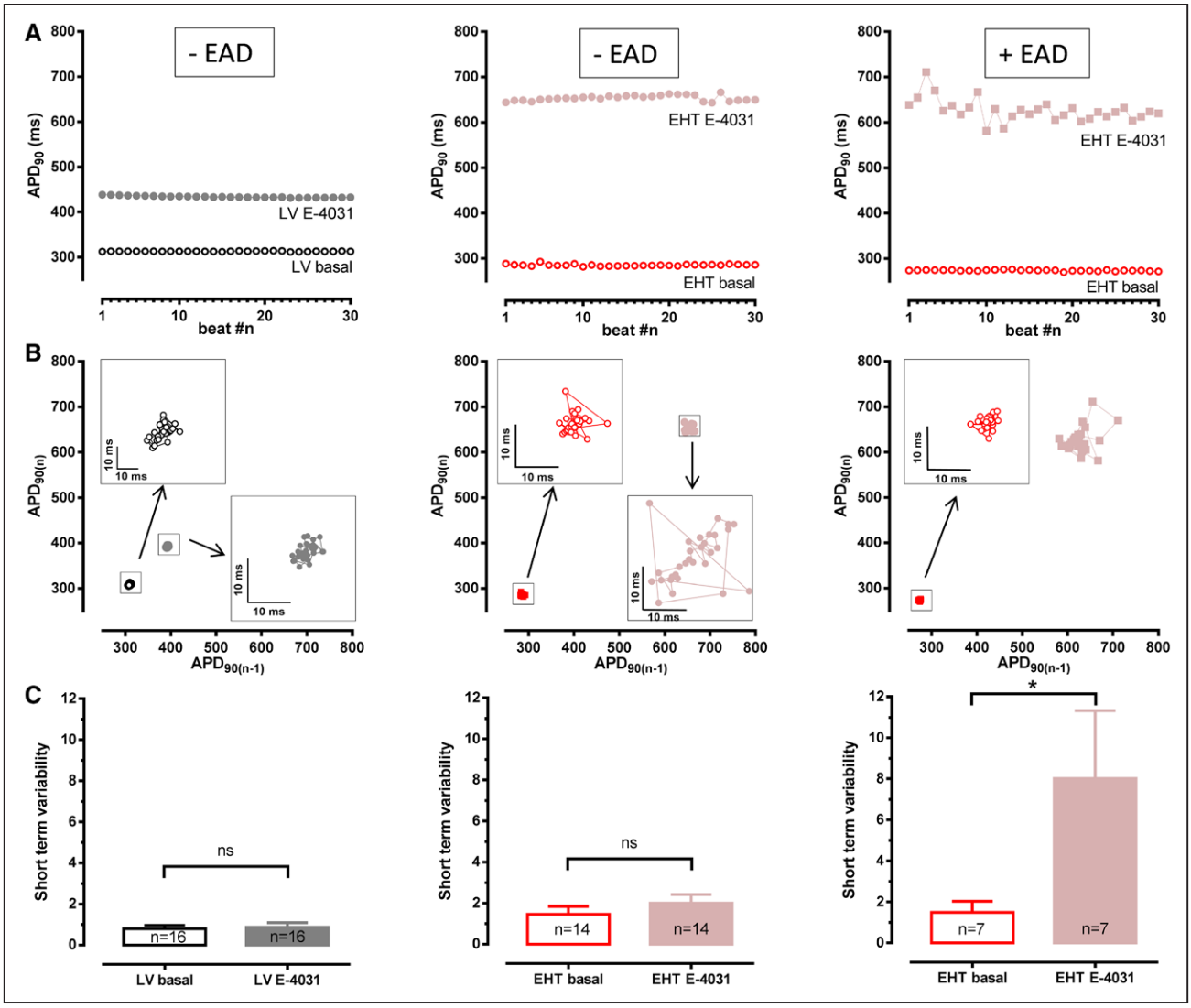

Figure 8. Prediction of early afterdepolarizations (EADs) by short-term variability (STV) of action potential duration at 90% repolarization (APD_{90}). **A**, Time course of APD_{90} at basal condition and in the presence of 1 µmol/L E-4031 for left ventricle (LV) and engineered heart tissue (EHT, in-house cell line C25) with (**right**) and without (**left/middle**) EADs, same groups for (**B** and **C**). **B**, Respective poincaré plots of APD_{90} with insets displaying data point at expanded scales. **C**, Quantification of STV of APD_{90} in the respective group. Mean±SEM of STV, **P*<0.05; paired *t* test. ns indicates nonsignificant.

hiPSC-CMs is controversial.[14,32–34] Here, we demonstrated for the first time that a reduction of spontaneous frequency by a low concentration of ivabradine is associated with a reduction of DD, suggesting a relevant contribution of I_f to pacemaking in hiPSC-CM in EHT. In the normal development of the heart, Ca^{2+}-clock pacemaking predominates the first phase of development, whereas the membrane clock's influence rises during development to the adult state.[35] If one interprets the strong dependence of spontaneous beating on ivabradine as a sign of dominance of the membrane clock over the Ca^{2+}-clock in EHT, this observation may indicate a later stage of maturation of hiPSC-CM. However, it should be noted that hiPSC-CM culture in EHT does not reduce the spontaneous rate per se,[12] and the definitive source of automaticity in EHT is difficult to identify.[14] Nevertheless, the omnipresent, ivabradine-sensitive DD and the ventricular-like repolarization fraction point to ventricular-like CMs with an abnormally high I_f.

Ivabradine does not affect AP shape in healthy[36] and failing LV (Figure IV in the Data Supplement). In contrast, ivabradine can prolong APs in canine LV,[36] when repolarization reserve is impaired. Despite the clear evidence for a smaller repolarization reserve in EHT than in LV, ivabradine did not affect AP shape, neither under basal conditions nor in the presence of E-4031. To avoid a potential bias by pretreating only EHT with ivabradine, we also performed experiments in LV with 300 nmol/L ivabradine and E-4031. As seen in EHT and LV, maximum E-4031–induced AP prolongation with or without ivabradine did not differ (Table IV in the Data Supplement). Therefore, we feel confident in the use of ivabradine to facilitate AP recordings in EHT at slow rates without reducing the repolarization reserve.

Contribution of I_{Kr} to APD Regulation in EHT

Block of I_{Kr} by E-4031 induced AP prolongation in both EHT and LV, starting just <0 mV of the membrane potential. Although half-effective concentration values did not differ between EHT and LV (both ≈3-fold lower than reported for human atrial tissue; 181 nmol/L[15]), the total effect was ≈2.5-fold higher in hiPSC-EHT. The pronounced prolongation on I_{Kr} inhibition in EHT can be mainly explained by the higher I_{Kr} [2,6,7,11,23,24] and I_{CaL} densities[21] in hiPSC-CM than in LV. Our in-silico modeling suggests that enhanced depolarizing and repolarizing currents in hiPSC-CM-EHTs are balancing each other under basal conditions. When I_{Kr} is blocked (either in the in-silico model or experimentally), this balance is abolished, and APs are markedly prolonged. Both the modeling data (Figure 7) and the experiments with verapamil (Figure 4) show that this prolongation is carried by a strong Ca^{2+} influx.

The inhibition of I_{Kr} shows a reverse use-dependence, which might be dangerous for class III antiarrhythmic compounds, such as sotalol. Many models like papillary muscles from guinea-pig[20] and rabbits[4] fail to demonstrate reverse use-dependence of I_{Kr} blockers. In contrast, hiPSC-CM displayed pronounced reverse use-dependence similar to LV, qualifying EHT as model to study bradycardia-associated EAD generation, which is the dominant trigger for TdP in the human heart.

Contribution of I_{Ks} to APD Regulation in EHT

There is no doubt about the relevance of I_{Ks} contribution to repolarization in human ventricle in vivo as LQT1 syndrome leads to life-threatening TdP arrhythmia. In stark contrast, under ex vivo conditions, I_{Ks} contribution to repolarization is difficult to demonstrate. Ex vivo measurements of human nonfailing LV showed that I_{Ks} does not contribute to repolarization under basal conditions.[2] Reducing the repolarization reserve by I_{Kr} block and the activation of β-AR was necessary to unmask a small increase in APD_{90} by I_{Ks} block,[19] which may be seen in line with the clinical effectiveness of sympathetic denervation to suppress TdP in LQT1 patients.[37] We could confirm this finding for failing LV and EHT (Figure 5). On the contrary, recent publications reported that APD of hiPSC-CM derived from LQT1 patients were markedly longer than those from control cell lines.[6,26] The reasons for this difference to normal human heart physiology (and our present data) are unknown, but the observation indicates a large nonphysiological contribution of I_{Ks} to repolarization in these hiPSC-CM cell lines or may result from the high variability in APD between control cell lines (Figure III in the Data Supplement).

EADs on I_{Kr} Block in EHT

EADs are one of the triggers initiating TdP in both genetic and drug-induced LQTS. Under ex vivo conditions, inhibition of I_{Kr} alone is not sufficient to induce EADs in human LV preparations[2,3] (and this study). Even the stimulation of β-AR in the presence of low extracellular potassium concentration was not sufficient to induce EADs in human LV[3] but in 30% of rabbit heart.[3] In our study, multiple interventions to reduce potassium conductance and activation of β-AR were necessary to induce EADs in LV (Figure 6 and Figure VI in the Data Supplement). In contrast, EADs developed in ≈50% of EHTs when I_{Kr} was blocked by 1 μmol/L E-4031 only. This finding again demonstrates an extraordinarily large contribution of I_{Kr} to electrical stability in hiPSC-CM[7] embedded in EHT. Unlike in LV, the occurrence of EADs in EHT was not restricted to extraordinarily long APD (Figure 6). As previously reported for canine heart,[16] we could confirm that STV works as a predictor of EAD development in EHT when I_{Kr} is blocked.

Isolated CMs are prone to develop EADs, limiting the specificity to predict clinically relevant TdP arrhythmia.[22] For instance, moxifloxacin is known to induce EADs in single cardiomyocytes but not in cardiac tissue or intact animals[22] and verapamil has no torsadogenic risk. The lack of EAD development in EHT on moxifloxacin and verapamil fits with clinical data and indicates a high specificity of hiPSC-EHTs in predicting proarrhythmic risk.

Potential Cellular Mechanisms for EADs

The high susceptibility of EHT to develop EADs indicates differences in the cellular electrophysiology when compared with LV. In a previous study, we found similar upstroke velocities that indicate physiological peak I_{Na}.[12] In the same report, we did not find late I_{Na} in hiPSC-CM, excluding this as a potential mechanism for EAD development. Ca^{2+} influx across the cell membrane is larger in hiPSC-CM, as I_{CaL} density is higher.[21] By blocking I_{CaL}, the pronounced AP prolongation by I_{Kr} block was diminished (Figure 4C and 4D) and EAD development prevented. Furthermore, I_{CaT}, which is absent in human adult LV CMs, is active in hiPSC-CMs.[21] However, its contribution to the total Ca^{2+} influx is much smaller than I_{CaL} (ratio, ≈1:50). In-silico investigation suggests that strong I_{CaL} density[21] in the hiPSC-CM contributes substantially to lowering the EAD threshold on I_{Kr} block, whereas reduced I_{K1} density and the contribution of I_{CaT} had only a small proarrhythmic effect (Figure 7D). The strong I_{Kr} current is suggested to be antiarrhythmic by counterbalancing strong I_{CaL} and by prohibiting early AP prolongation and EAD development by I_{Kr} block. However, when the repolarizing force of strong I_{Kr} is abrogated by a higher degree of I_{Kr} block, inward currents can be large enough to generate the EADs.

Potential Structural Mechanisms for EADs

Although the EHT format supports the structural maturation of hiPSC-CM to a more rod-shaped form and better end-to-end cell contacts,[12] the cell density in EHT is still lower than in adult cardiac tissue and may cause reduced coupling of CM. After the source-sink theory,[38] lower coupling means less (hyperpolarizing) sink. Assuming a heterogeneous EAD development (as the source) on I_{Kr} block in individual cells, this may explain the high susceptibility to EADs in EHT compared with LV because coupling (as the sink)[38] can buffer less in EHT than in LV.

EHT as a Model for PFs?

Strong AP prolongation and high susceptibility to the development of EADs on I_{Kr} block are classic hallmarks of PF. Therefore, PFs but not papillary muscles are used in safety pharmacology to unmask even small risks of arrhythmogenicity.[4,5] EHTs developed EADs on I_{Kr} block with a similar incidence (50%) as reported for rabbit and canine PF (40%–80%),[4,5,39] whereas LV preparations from rabbit[4] and human[3,19] did not. Enhanced I_f, I_{CaL}, and I_{CaT}[40,41] might be responsible for this difference, all of which would be expected to contribute to ivabradine-sensitive DD[36], strong AP prolongation and EAD development on I_{Kr} inhibition. In fact, the same features were observed in the present study in hiPSC-CM EHTs, suggesting that this new model might be as sensitive as PFs to predict EAD development in (drug induced) LQTS. Detailed comparative studies are necessary to investigate whether hiPSC-CMs in EHT share the basic electrophysiological peculiarities of PF CMs.

Limitations

Current densities for in-silico analysis were taken from published data for hiPSC-CM cultured isolated or in monolayers (Table IV in the Data Supplement). Differences in current densities between CM cultured in EHT or monolayer, as known for I_{Na},[12] cannot be excluded. All 3 iPS cell lines were generated from female donors. It remains unclear whether hiPSC-CMs reflect the well-known sex differences of AP. LV tissue was obtained from patients with aortic valve disease or heart failure as we do not have access to LV tissue of healthy humans (Table V in the Data Supplement). Thus, potential disease-specific differences in AP parameters cannot be excluded.

Conclusions

We have characterized the impact of the 2 repolarizing currents of LQT1 and LQT2 in hiPSC-CM–based EHT compared with human ventricular tissue. The exaggerated AP prolongation and the high susceptibility to EADs of hiPSC-CM on I_{Kr} block indicate hiPSC-CM as a sensitive test system for QT prolongation and arrhythmic triggers in I_{Kr} assays. hiPSC-CM in EHT might serve as a sensitive and specific model to study the individual response to I_{Kr} block also in respect to monogenic arrhythmogenic heart disease.

ARTICLE INFORMATION

Received November 13, 2017; accepted May 8, 2018.

The Data Supplement is available at https://www.ahajournals.org/journal/circep/doi/suppl/10.1161/CIRCEP.117.006035.

Correspondence

Marc D. Lemoine, MD, Department of Experimental Pharmacology and Toxicology, University Medical Center, Hamburg-Eppendorf, Martinistrasse 52, 20246 Hamburg, Germany, E-mail m.lemoine@uke.de or Torsten Christ, MD, Department of Experimental Pharmacology and Toxicology, University Medical Center, Hamburg-Eppendorf, Martinistrasse 52, 20246 Hamburg, Germany, E-mail t.christ@uke.de

Affiliations

Department of Cardiology-Electrophysiology (M.D.L., S.W.) and Department of Cardiovascular Surgery (E.G.), University Heart Center, Hamburg-Eppendorf, Germany. Department of Experimental Pharmacology and Toxicology, University Medical Center, Hamburg-Eppendorf, Germany (M.D.L., T.K., M.P., M.L.S., A.H., T.E., T.C.). DZHK (German Center for Cardiovascular Research), Partner Site Hamburg/Kiel/Lübeck, Germany (M.D.L., T.K., M.P., M.L.S., S.W., A.H., T.E., T.C.). A.I. Virtanen Institute for Molecular Sciences, University of Eastern Finland, Kuopio (J.T.K.). BioMediTech Institute and Faculty of Biomedical Sciences and Engineering, Tampere University of Technology, Finland (J.T.K.).

Acknowledgments

We gratefully acknowledge expert technical advice and help in providing engineered heart tissues (EHTs) and left ventricular (LV) tissue from Benjamin Kloth, Sharia Iqbal, Umber Saleem, Ingra Mannhardt, Anika Knaust, Tessa Werner, Marta Lemme, Klaus Söhren, Thomas Schulze, Birgit Klampe, Elisabeth Krämer, Aya Domke-Shibamiya, and Sandra Laufer. We also thank Alessandra Moretti and Dennis Schade for their kind contribution of materials, Herbert Himmel for expert advice in electrophysiological safety studies, and Jennifer N. Lohr for useful comments on the article, as well as language editing and proofreading.

Sources of Funding

This work was supported by the German Centre for Cardiovascular Research (DZHK), German Ministry of Education and Research, AFib-TrainNet (675351 to Drs Christ and Eschenhagen), and the European Research Council Advanced Grant (IndivuHeart to Dr Eschenhagen). Dr Lemoine was supported by the German Centre for Cardiovascular Research (DZHK rotation grant) and Dr Koivumäki by the Finish Foundation for Cardiovascular Research and Paavo Nurmi Foundation.

Disclosures

Drs Hansen and Eschenhagen are cofounders of EHT Technologies GmbH, Hamburg. The other authors report no conflicts.

REFERENCES

1. Tester DJ, Will ML, Haglund CM, Ackerman MJ. Compendium of cardiac channel mutations in 541 consecutive unrelated patients referred for long QT syndrome genetic testing. *Heart Rhythm*. 2005;2:507–517. doi: 10.1016/j.hrthm.2005.01.020.
2. Jost N, Virág L, Comtois P, Ordög B, Szuts V, Seprényi G, Bitay M, Kohajda Z, Koncz I, Nagy N, Szél T, Magyar J, Kovács M, Puskás LG, Lengyel C,

Wettwer E, Ravens U, Nánási PP, Papp JG, Varró A, Nattel S. Ionic mechanisms limiting cardiac repolarization reserve in humans compared to dogs. *J Physiol*. 2013;591:4189–4206. doi: 10.1113/jphysiol.2013.261198.
3. Vermeulen JT, McGuire MA, Opthof T, Coronel R, de Bakker JM, Klöpping C, Janse MJ. Triggered activity and automaticity in ventricular trabeculae of failing human and rabbit hearts. *Cardiovasc Res*. 1994;28:1547–1554.
4. Lu HR, Vlaminckx E, Teisman A, Gallacher DJ. Choice of cardiac tissue plays an important role in the evaluation of drug-induced prolongation of the QT interval *in vitro* in rabbit. *J Pharmacol Toxicol Methods*. 2005;52:90–105. doi: 10.1016/j.vascn.2005.04.007.
5. Jonsson MK, Duker G, Tropp C, Andersson B, Sartipy P, Vos MA, van Veen TA. Quantified proarrhythmic potential of selected human embryonic stem cell-derived cardiomyocytes. *Stem Cell Res*. 2010;4:189–200. doi: 10.1016/j.scr.2010.02.001.
6. Moretti A, Bellin M, Welling A, Jung CB, Lam JT, Bott-Flügel L, Dorn T, Goedel A, Höhnke C, Hofmann F, Seyfarth M, Sinnecker D, Schömig A, Laugwitz KL. Patient-specific induced pluripotent stem-cell models for long-QT syndrome. *N Engl J Med*. 2010;363:1397–1409. doi: 10.1056/NEJMoa0908679.
7. Itzhaki I, Maizels L, Huber I, Zwi-Dantsis L, Caspi O, Winterstern A, Feldman O, Gepstein A, Arbel G, Hammerman H, Boulos M, Gepstein L. Modelling the long QT syndrome with induced pluripotent stem cells. *Nature*. 2011;471:225–229. doi: 10.1038/nature09747.
8. Malan D, Zhang M, Stallmeyer B, Müller J, Fleischmann BK, Schulze-Bahr E, Sasse P, Greber B. Human iPS cell model of type 3 long QT syndrome recapitulates drug-based phenotype correction. *Basic Res Cardiol*. 2016;111:14. doi: 10.1007/s00395-016-0530-0.
9. Liang P, Sallam K, Wu H, Li Y, Itzhaki I, Garg P, Zhang Y, Vermglinchan V, Lan F, Gu M, Gong T, Zhuge Y, He C, Ebert AD, Sanchez-Freire V, Churko J, Hu S, Sharma A, Lam CK, Scheinman MM, Bers DM, Wu JC. Patient-specific and genome-edited induced pluripotent stem cell-derived cardiomyocytes elucidate single-cell phenotype of Brugada syndrome. *J Am Coll Cardiol*. 2016;68:2086–2096. doi: 10.1016/j.jacc.2016.07.779.
10. Doss MX, Di Diego JM, Goodrow RJ, Wu Y, Cordeiro JM, Nesterenko VV, Barajas-Martínez H, Hu D, Urrutia J, Desai M, Treat JA, Sachinidis A, Antzelevitch C. Maximum diastolic potential of human induced pluripotent stem cell-derived cardiomyocytes depends critically on I(Kr). *PLoS One*. 2012;7:e40288. doi: 10.1371/journal.pone.0040288.
11. Ma J, Guo L, Fiene SJ, Anson BD, Thomson JA, Kamp TJ, Kolaja KL, Swanson BJ, January CT. High purity human-induced pluripotent stem cell-derived cardiomyocytes: electrophysiological properties of action potentials and ionic currents. *Am J Physiol Heart Circ Physiol*. 2011;301:H2006–H2017. doi: 10.1152/ajpheart.00694.2011.
12. Lemoine MD, Mannhardt I, Breckwoldt K, Prondzynski M, Flenner F, Ulmer B, Hirt MN, Neuber C, Horváth A, Kloth B, Reichenspurner H, Willems S, Hansen A, Eschenhagen T, Christ T. Human iPSC-derived cardiomyocytes cultured in 3D engineered heart tissue show physiological upstroke velocity and sodium current density. *Sci Rep*. 2017;7:5464. doi: 10.1038/s41598-017-05600-w.
13. Horváth A, Lemoine MD, Löser A, Mannhardt I, Flenner F, Uzun AU, Neuber C, Breckwoldt K, Hansen A, Girdauskas E, Reichenspurner H, Willems S, Jost N, Wettwer E, Eschenhagen T, Christ T. Low resting membrane potential and low inward rectifier potassium currents are not inherent features of hiPSC-derived cardiomyocytes. *Stem Cell Reports*. 2018;10:822–833. doi: 10.1016/j.stemcr.2018.01.012.
14. Mannhardt I, Breckwoldt K, Letuffe-Brenière D, Schaaf S, Schulz H, Neuber C, Benzin A, Werner T, Eder A, Schulze T, Klampe B, Christ T, Hirt MN, Huebner N, Moretti A, Eschenhagen T, Hansen A. Human engineered heart tissue: analysis of contractile force. *Stem Cell Reports*. 2016;7:29–42. doi: 10.1016/j.stemcr.2016.04.011.
15. Wettwer E, Christ T, Endig S, Rozmaritsa N, Matschke K, Lynch JJ, Pourrier M, Gibson JK, Fedida D, Knaut M, Ravens U. The new antiarrhythmic drug vernakalant: ex vivo study of human atrial tissue from sinus rhythm and chronic atrial fibrillation. *Cardiovasc Res*. 2013;98:145–154. doi: 10.1093/cvr/cvt006.
16. Thomsen MB, Verduyn SC, Stengl M, Beekman JD, de Pater G, van Opstal J, Volders PG, Vos MA. Increased short-term variability of repolarization predicts d-sotalol-induced torsades de pointes in dogs. *Circulation*. 2004;110:2453–2459. doi: 10.1161/01.CIR.0000145162.64183.C8.
17. Grandi E, Pasqualini FS, Bers DM. A novel computational model of the human ventricular action potential and Ca transient. *J Mol Cell Cardiol*. 2010;48:112–121. doi: 10.1016/j.yjmcc.2009.09.019.
18. Hondeghem LM, Snyders DJ. Class III antiarrhythmic agents have a lot of potential but a long way to go. Reduced effectiveness and dangers of reverse use dependence. *Circulation*. 1990;81:686–690.
19. Jost N, Virág L, Bitay M, Takács J, Lengyel C, Biliczki P, Nagy Z, Bogáts G, Lathrop DA, Papp JG, Varró A. Restricting excessive cardiac action potential and QT prolongation: a vital role for IKs in human ventricular muscle. *Circulation*. 2005;112:1392–1399. doi: 10.1161/CIRCULATIONAHA.105.550111.
20. Ohler A, Ravens U. Effects of E-4031, almokalant and tedisamil on postrest action potential duration of human papillary muscles. *J Pharmacol Exp Ther*. 1994;270:460–465.
21. Uzun AU, Mannhardt I, Breckwoldt K, Horváth A, Johannsen SS, Hansen A, Eschenhagen T, Christ T. Ca(2+)-Currents in human induced pluripotent stem cell-derived cardiomyocytes effects of two different culture conditions. *Front Pharmacol*. 2016;7:300. doi: 10.3389/fphar.2016.00300.
22. Nalos L, Varkevisser R, Jonsson MK, Houtman MJ, Beekman JD, van der Nagel R, Thomsen MB, Duker G, Sartipy P, de Boer TP, Peschar M, Rook MB, van Veen TA, van der Heyden MA, Vos MA. Comparison of the IKr blockers moxifloxacin, dofetilide and E-4031 in five screening models of pro-arrhythmia reveals lack of specificity of isolated cardiomyocytes. *Br J Pharmacol*. 2012;165:467–478. doi: 10.1111/j.1476-5381.2011.01558.x.
23. Magyar J, Iost N, Körtvély A, Bányász T, Virág L, Szigligeti P, Varró A, Opincariu M, Szécsi J, Papp JG, Nánási PP. Effects of endothelin-1 on calcium and potassium currents in undiseased human ventricular myocytes. *Pflugers Arch*. 2000;441:144–149. doi: 10.1007/s004240000400.
24. Iost N, Virág L, Opincariu M, Szécsi J, Varró A, Papp JG. Delayed rectifier potassium current in undiseased human ventricular myocytes. *Cardiovasc Res*. 1998;40:508–515.
25. Egashira T, Yuasa S, Suzuki T, Aizawa Y, Yamakawa H, Matsuhashi T, Ohno Y, Tohyama S, Okata S, Seki T, Kuroda Y, Yae K, Hashimoto H, Tanaka T, Hattori F, Sato T, Miyoshi S, Takatsuki S, Murata M, Kurokawa J, Furukawa T, Makita N, Aiba T, Shimizu W, Horie M, Kamiya K, Kodama I, Ogawa S, Fukuda K. Disease characterization using LQTS-specific induced pluripotent stem cells. *Cardiovasc Res*. 2012;95:419–429. doi: 10.1093/cvr/cvs206.
26. Zhang M, D'Aniello C, Verkerk AO, Wrobel E, Frank S, Ward-van Oostwaard D, Piccini I, Freund C, Rao J, Seebohm G, Atsma DE, Schulze-Bahr E, Mummery CL, Greber B, Bellin M. Recessive cardiac phenotypes in induced pluripotent stem cell models of Jervell and Lange-Nielsen syndrome: disease mechanisms and pharmacological rescue. *Proc Natl Acad Sci USA*. 2014;111:E5383–E5392. doi: 10.1073/pnas.1419553111.
27. Virág L, Iost N, Opincariu M, Szolnoky J, Szécsi J, Bogáts G, Szenohradszky P, Varró A, Papp JG. The slow component of the delayed rectifier potassium current in undiseased human ventricular myocytes. *Cardiovasc Res*. 2001;49:790–797.
28. O'Hara T, Virág L, Varró A, Rudy Y. Simulation of the undiseased human cardiac ventricular action potential: model formulation and experimental validation. *PLoS Comput Biol*. 2011;7:e1002061. doi: 10.1371/journal.pcbi.1002061.
29. Herron TJ, Rocha AM, Campbell KF, Ponce-Balbuena D, Willis BC, Guerrero-Serna G, Liu Q, Klos M, Musa H, Zarzoso M, Bizy A, Furness J, Anumonwo J, Mironov S, Jalife J. Extracellular matrix-mediated maturation of human pluripotent stem cell-derived cardiac monolayer structure and electrophysiological function. *Circ Arrhythm Electrophysiol*. 2016;9:e003638. doi: 10.1161/CIRCEP.113.003638.
30. Schram G, Pourrier M, Wang Z, White M, Nattel S. Barium block of Kir2 and human cardiac inward rectifier currents: evidence for subunit-heteromeric contribution to native currents. *Cardiovasc Res*. 2003;59:328–338.
31. Feaster TK, Cadar AG, Wang L, Williams CH, Chun YW, Hempel JE, Bloodworth N, Merryman WD, Lim CC, Wu JC, Knollmann BC, Hong CC. Matrigel mattress: a method for the generation of single contracting human-induced pluripotent stem cell-derived cardiomyocytes. *Circ Res*. 2015;117:995–1000. doi: 10.1161/CIRCRESAHA.115.307580.
32. Zhang XH, Wei H, Šarić T, Hescheler J, Cleemann L, Morad M. Regionally diverse mitochondrial calcium signaling regulates spontaneous pacing in developing cardiomyocytes. *Cell Calcium*. 2015;57:321–336. doi: 10.1016/j.ceca.2015.02.003.
33. Kim JJ, Yang L, Lin B, Zhu X, Sun B, Kaplan AD, Bett GC, Rasmusson RL, London B, Salama G. Mechanism of automaticity in cardiomyocytes derived from human induced pluripotent stem cells. *J Mol Cell Cardiol*. 2015;81:81–93. doi: 10.1016/j.yjmcc.2015.01.013.
34. Chen Z, Xian W, Bellin M, Dorn T, Tian Q, Goedel A, Dreizehnter L, Schneider CM, Ward-van Oostwaard D, Ng JK, Hinkel R, Pane LS, Mummery CL, Lipp P, Moretti A, Laugwitz KL, Sinnecker D. Subtype-specific promoter-driven action potential imaging for precise disease modelling and drug

testing in hiPSC-derived cardiomyocytes. *Eur Heart J*. 2017;38:292–301. doi: 10.1093/eurheartj/ehw189.
35. Louch WE, Koivumäki JT, Tavi P. Calcium signalling in developing cardiomyocytes: implications for model systems and disease. *J Physiol*. 2015;593:1047–1063. doi: 10.1113/jphysiol.2014.274712.
36. Koncz I, Szél T, Bitay M, Cerbai E, Jaeger K, Fülöp F, Jost N, Virág L, Orvos P, Tálosi L, Kristóf A, Baczkó I, Papp JG, Varró A. Electrophysiological effects of ivabradine in dog and human cardiac preparations: potential antiarrhythmic actions. *Eur J Pharmacol*. 2011;668:419–426. doi: 10.1016/j.ejphar.2011.07.025.
37. Schwartz PJ. Cardiac sympathetic denervation to prevent life-threatening arrhythmias. *Nat Rev Cardiol*. 2014;11:346–353. doi: 10.1038/nrcardio.2014.19.
38. Xie Y, Sato D, Garfinkel A, Qu Z, Weiss JN. So little source, so much sink: requirements for afterdepolarizations to propagate in tissue. *Biophys J*. 2010;99:1408–1415. doi: 10.1016/j.bpj.2010.06.042.
39. Nattel S, Quantz MA. Pharmacological response of quinidine induced early afterdepolarisations in canine cardiac Purkinje fibres: insights into underlying ionic mechanisms. *Cardiovasc Res*. 1988;22:808–817.
40. Tseng GN, Boyden PA. Multiple types of Ca2+ currents in single canine Purkinje cells. *Circ Res*. 1989;65:1735–1750.
41. Gaborit N, Le Bouter S, Szuts V, Varro A, Escande D, Nattel S, Demolombe S. Regional and tissue specific transcript signatures of ion channel genes in the non-diseased human heart. *J Physiol*. 2007;582(pt 2):675–693. doi: 10.1113/jphysiol.2006.126714.